HYDROLOGICAL PROCESSES
Hydrol. Process. **19**, 1333–1353 (2005)
Published online 8 December 2004 in Wiley InterScience (www.interscience.wiley.com). DOI: 10.1002/hyp.5567

Understanding and modeling basin hydrology: interpreting the hydrogeological signature

R. E. Beighley,[1]* T. Dunne[2] and J. M. Melack[2]

[1] *Institute for Computational Earth System Science, University of California, Santa Barbara, CA 93106, USA*
[2] *Bren School of Environmental Science and Management, University of California, Santa Barbara, CA 93106, USA*

Abstract:

Basin landscapes possess an identifiable spatial structure, fashioned by climate, geology and land use, that affects their hydrologic response. This structure defines a basin's hydrogeological signature and corresponding patterns of runoff and stream chemistry. Interpreting this signature expresses a fundamental understanding of basin hydrology in terms of the dominant hydrologic components: surface, interflow and groundwater runoff. Using spatial analysis techniques, spatially distributed watershed characteristics and measurements of rainfall and runoff, we present an approach for modelling basin hydrology that integrates hydrogeological interpretation and hydrologic response unit concepts, applicable to both new and existing rainfall-runoff models. The benefits of our modelling approach are a clearly defined distribution of dominant runoff form and behaviour, which is useful for interpreting functions of runoff in the recruitment and transport of sediment and other contaminants, and limited over-parameterization. Our methods are illustrated in a case study focused on four watersheds (24 to 50 km^2) draining the southern coast of California for the period October 1988 though to September 2002. Based on our hydrogeological interpretation, we present a new rainfall-runoff model developed to simulate both surface and subsurface runoff, where surface runoff is from either urban or rural surfaces and subsurface runoff is either interflow from steep shallow soils or groundwater from bedrock and coarse-textured fan deposits. Our assertions and model results are supported using streamflow data from seven US Geological Survey stream gauges and measured stream silica concentrations from two Santa Barbara Channel–Long Term Ecological Research Project sampling sites. Copyright © 2004 John Wiley & Sons, Ltd.

KEY WORDS geographic information systems; hydrology; hydrologic response unit; interflow; mediterranean climate; model; runoff; streamflow; subsurface; watershed response

INTRODUCTION

It is possible to organize a basin into discrete units possessing similar rainfall-runoff characteristics by integrating spatially distributed climate, geology, land use, soils and topographic data, and isolating areas that are approximately homogeneous in their hydrologic properties (Becker and Braun, 1999; Beven, 2001). The process of merging the landscape into separate hydrologic response units (HRUs) is a common method for reducing model complexity and spatially distributed data requirements in basin-scale models: HEC-HMS (USACE, 2000), HSPF (Donigian *et al*., 1995), and SWAT (Arnold *et al*., 1995). Once HRUs are defined, the rainfall-runoff processes within each unit must be identified and parameterized. Generally, the runoff processes are characterized for the watershed as a whole and each HRU is parameterized for all processes (i.e. overland, interflow and groundwater runoff). Numerous research efforts have focused on integrating geographic information systems (GISs), hydrologic models and spatial/temporal databases to expedite and enhance the delineation and parameterization processes (Olivera, 2001; Moglen and Kosicki, 2000; Miller *et al*., 2002). However, interpreting the role of individual HRUs in structuring the dominant hydrologic components (i.e. overland, interflow and groundwater runoff) at the basin scale is not part of standard modelling procedures.

* Correspondence to: R. E. Beighley, San Diego State University, Department of Civil and Environmental Engineering, 5500 Campanile Drive, San Diego, CA 92182-1324, USA. E-mail: beighley@egr.sdsu.edu

Received 28 May 2003
Accepted 20 February 2004

Though this interpretation may not be necessary for studies primarily focused on combined streamflow, such as estimating peak flood flows for hydraulic design or annual runoff for water supply studies, it can provide valuable insight to multidisciplinary environmental research questions dependent upon runoff mechanisms and pathways, such as stream water quality, non-point-source pollution and surface–groundwater interactions.

Generally, basin-scale modelling approaches focus on parameterizing HRU-scale processes corresponding to a single conceptual model representing the watershed's hydrologic cycle. For example, if it is presumed that streamflow at the watershed outlet is comprised of surface, shallow soil 'interflow' and groundwater runoff, then each HRU will be parameterized for all three runoff components. This concept assumes that the parameterization process incorporates the spatial variability of land use, soils and topography characteristics to approximate the runoff mechanisms in each HRU. However, this may result in parameterizing a non-existent process. For example, steep mountainous areas with permeable soils and shallow bedrock will primarily produce interflow (Hewlett and Hibbert, 1963; Harr, 1977). In contrast, mildly sloping areas with deep, permeable soils or sediments will likely produce only groundwater runoff (Farvolden, 1963). Trying to parameterize and calibrate all three sources of runoff in the above two cases may result in inappropriate parameter sets and/or a misrepresentation of the actual runoff mechanisms and flow pathways.

However, it is possible to use information on the spatial structure of the landscape to identify regions of similar runoff characteristics, which can then be combined with existing HRU concepts to overcome the problem of over-parameterization and provide a process-oriented subdivision of a basin (Hellie *et al*., 2002). The spatial structure of the landscape defines a basin's hydrogeological signature and corresponding patterns of runoff and stream chemistry. Interpreting this signature yields a fundamental understanding of basin hydrology in terms of the dominant hydrologic components: surface, interflow and groundwater runoff. Using spatial analysis techniques, it is possible to identify locations throughout a basin that have similar hydrologic characteristics and which are likely to exhibit similar runoff processes (Peschke *et al*., 1999). Mapping such interpretations of dominant runoff processes onto the landscape is a valuable step that is often not performed. By combining runoff component mapping (i.e. hydrogeological interpretation) with standard HRU concepts, it is possible to enhance the selection of appropriate modelling approaches and limit unnecessary parameterizations.

Other studies have investigated similar concepts, in that they desired to simplify the rainfall-runoff process by interpreting the underlying basin signature: Grayson *et al*. (2002) provide an overview of recent advances in the use of spatial patterns for defining spatial structure and improving distributed hydrologic modeling; Woods (2002) highlights the lack of a quantitative reliance on spatial views of hydrologic data; Grayson and Bloschl (2000) introduce the 'dominant processes concept', highlighting the need to identify dominant processes in different hydrologic settings and at different spatial and temporal scales to aid in selecting the appropriate model structure for given modelling objectives; Jakeman and Hornberger (1993) focused specifically on the rainfall-runoff signature to discern the structure of a two-component (quick and slow) runoff model; Wooldridge *et al*. (2002) refer to the importance of the hydrologic signature, in formulating their modified quasi-distributed VIC hydrologic model (Liang *et al*., 1994), which combines both land use and streamflow characteristics.

In this paper, we present an approach for modelling basin hydrology that integrates hydrogeological interpretation and HRU concepts, applicable for both existing and new rainfall-runoff models. We focus on determining the fundamental hydrologic components of a basin and mapping areas that are expected to exhibit similar runoff processes and pathways. By combining the hydrogeological signature with HRU concepts, we present a new basin-scale model that simulates streamflow from three sources of runoff: surface, interflow and groundwater. A case study, of four watersheds draining the southern coast of California near Santa Barbara, is presented to demonstrate the hydrogeological interpretation and modelling approach. The benefits of our enhanced HRU modelling approach are: (1) a clearly defined distribution of dominant runoff form and behaviour (i.e. provision of a more informative assessment of runoff processes and pathways resulting in a more powerful field evaluation); and (2) limited over-parameterization (i.e. reduction of the parameterization

and calibration of non-existent processes, while providing physically meaningful, quantitative measures to aid in characterizing the inferred processes).

HYDROGEOLOGICAL INTERPRETATION APPROACH

Accurately interpreting the dominant runoff characteristics of a watershed (i.e. hydrogeological signature) requires both qualitative and quantitative assessments of streamflow, precipitation and spatially distributed watershed data. The combination of data sources is required because measured streamflow alone is not sufficient for determining the spatial distribution of runoff components (i.e. runoff mechanisms and pathways) that comprise channel streamflow. Measured streamflow reflects the flux of water passing through a given channel cross-section, and thus represents the integration of all upstream rainfall-runoff processes occurring through paths which themselves have probability density functions of interacting hydrogeological properties (such as cross-sectional area, length, hydraulic conductivity, porosity, and antecedent water content). Although it is possible to discern primary streamflow components such as surface, interflow and groundwater (or event and pre-event water) using hydrograph separation techniques (Gremillion *et al*., 2000; Hoeg *et al*., 2000; Ladouche *et al*., 2001), the spatial distribution for the origin and contribution of the primary components cannot be known without an extensive internal gauging network. Meanwhile, modelling rainfall-runoff response using fully distributed or spatially averaged (HRU) approaches requires all runoff mechanisms and pathways to be defined throughout a watershed.

Inferring the spatial distribution of runoff processes and pathways is the focus of our work. Our hydrogeological interpretation procedure is intended to augment standard HRU modelling concepts by providing: a clearly defined distribution of dominate sources or runoff (i.e. providing testable hypotheses of runoff mechanisms and pathways); limited over-parameterization and calibration; a fundamental conceptualization of runoff sources useful for interpreting water quality signatures. Our approach has two parts: (1) mapping evidence of dominant hydrologic processes and (2) associating predefined HRUs with their corresponding runoff components. For completeness, we present our procedure in Figure 1, described below, as a series of six steps starting with defining HRUs.

First, obtain spatially distributed data for known drainage features (e.g. stream locations and storm sewers), geology, land use, precipitation, soils and topography, and process the elevation data to determine local gradients, flow directions and the corresponding drainage accumulation network. Next, select a threshold drainage area that corresponds to the know stream locations, subdivide the watershed at all junctions within this inferred network, and quantify the spatial patterns of hydrologic characteristics (such as depth to bedrock, distribution of land uses, mean annual rainfall, elevation, local gradient, and soils types/textures) within and between each sub-area. Then, assess the spatial variation of hydrologic properties within and between sub-areas relative to the research goals and objectives. If a more or less detailed drainage network is required, then modify the inferred drainage network (i.e. threshold drainage area) as needed. If the inferred drainage network and corresponding sub-areas are appropriate, then the HRUs are defined as the delineated sub-areas.

Once the HRUs have been defined, obtain available streamflow and rainfall data, and evaluate the major rainfall-runoff characteristics such as initial storage (i.e. delay between rainfall and runoff), runoff−rainfall ratios for storms, seasonality, streamflow recession rates. Develop preliminary hypotheses for potential runoff mechanisms and pathways within the watershed. Next, evaluate the available spatially distributed watershed data (climatic conditions, infiltration capacities, known bedrock layers, land use, slopes, soil texture, etc.) for uniqueness in space, and develop quantitative spatial measures to partition the watershed into regions of similar runoff behaviour using spatial data characteristics, preliminary runoff hypotheses, and fundamental hydrologic theories. Finally, assign the appropriate runoff processes to each HRU using the spatial distribution of the inferred dominant runoff mechanisms and pathways. Proceed with the parameterization and calibration process, while maintaining focus on the individual runoff processes. For example, it may be possible to use similar values and/or adjustments for model variables based on the assumed runoff components (i.e. focus the

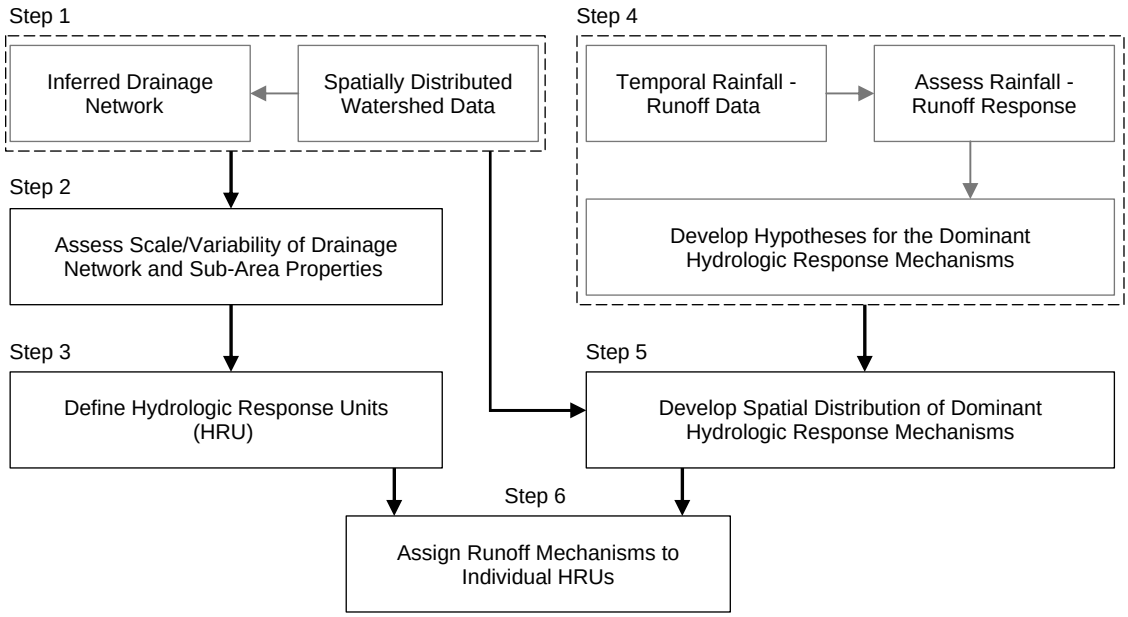

Figure 1. Hydrogeological interpretation procedure for assigning runoff mechanisms to individual HRUs

calibration process on runoff components rather than individual HRU parameters), which provides a rational and defensible means of reducing the number of parameterization and calibration parameters.

CASE STUDY

To illustrate our approach, we present a study of four watersheds, i.e. San Jose, Atascadero, Arroyo Burro and Mission Creeks, draining the southern coast of California between Goleta and Santa Barbara into the Pacific Ocean (i.e. Santa Barbara Channel; Figure 2). Their drainage areas range from 24 to 50 km^2, and their topographies are representative of coastal watersheds draining into the Santa Barbara Channel from the Santa Ynez Mountains (approximately 50 coastal watersheds ranging in size from <10 km^2 to ~ 500 km^2), with mountainous headwaters and mildly sloping coastal plains separated by narrow foothills.

The Mediterranean climate of the watersheds concentrates more than 80% of the annual rainfall in winter (December–March). The south-sloping orientation of the watersheds, the flow of moisture from south-southwest during winter storms, and the steep mountainous terrain contribute to significant orographic precipitation (NOAA, 2001). The average annual coastal plain precipitation over the past 40 years was approximately 50 cm (ranging between years from 20 to 120 cm) but rose to about 85 cm (ranging from 30 to 225 cm) in the mountains.

The type and distribution of the land uses within each watershed is consistent with the region's spatial development pattern: urbanization from Santa Barbara is expanding west towards Goleta and upslope into the rural foothills. From east to west, the watersheds tend to contain more agricultural and range/brush lands and less urban and forested lands. In the four study watersheds, 1998 land-use conditions range from 16 to 50% urban, 1 to 20% agricultural, 40 to 62% shrub/brush, and 2 to 9% forested (Table I). Within each watershed, the topographic characteristics are clearly correlated with land-use conditions: mountains are covered with shrub/brush, foothills contain agricultural lands, and coastal plains are urbanized.

There are seven US Geological Survey (USGS) stream gauges within the study region, generally distributed as upper and outlet gauges within each watershed (Figure 2). In addition, hourly water quality data from

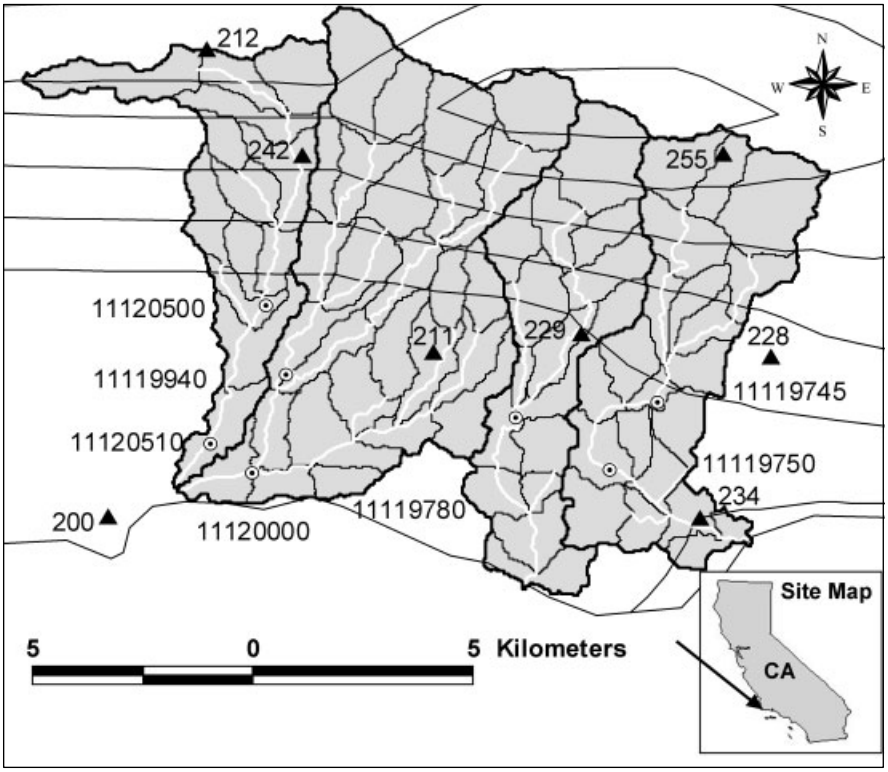

Figure 2. San Jose, Atascadero, Arroyo Burro, and Mission Creek watersheds (from left to right outlined in bold black), with sub-catchment areas (outlined in black), stream locations (white), stream gauge locations (circles), precipitation gauge locations (triangles), and 5 cm annual PRISM precipitation contours increasing from 40 cm at the outlet of Mission Creek to 70 cm in the headwaters of Atascadero and Arroyo Burro watersheds

Table I. Watershed land-use conditions in 1998

Watershed	Area (km^2)	Urban (%)	Agricultural (%)	Shrub/brush (%)	Forested (%)
San Jose	25	16	20	62	2
Atascadero	50	39	11	45	5
Arroyo Burro	24	40	6	45	9
Mission	30	50	1	41	8

water year 2001 are available for the outlets of Arroyo Burro and Mission Creek watersheds as part of the Santa Barbara Channel–Long Term Ecological Research Project (SBC–LTER). Table II provides gauging information and drainage-area characteristics for the seven USGS stream gauges. Precipitation is characterized by eight rainfall gauges operated by Santa Barbara County Public Works Department (Figure 2). Our case study assimilates the gauging records from the 14 year period October 1988 though to September 2002.

Hydrogeological interpretation

The primary sources of spatial data used were: topography, known drainage network (i.e. streams and storm sewers), hydrologic soil characteristics, land use, and long-term precipitation. Topography was derived from USGS digital elevation models (DEMs) with a spatial resolution of 30 m × 30 m grid cells. The known drainage network was a combination of stream locations (National Hydrography Dataset, 1999) and storm

Table II. USGS stream gauge information

USGS ID	Creek name	Area (km^2)	Relief (m)	Period of record	Mean daily flow ($m^3\ s^{-1}$)
11119745	Mission	17·1	900	1 Oct 1983–current	0·10
11119750	Mission	21·7	940	1 Oct 1970–current	0·09
11119780	Arroyo Burro	17·2	1080	1 Oct 1970–30 Sep 1993	0·06
11119940	Maria Ygnacio	16·6	1130	1 Oct 1970–current	0·06
11120000	Atascadero	49·0	1170	1 Oct 1941–current	0·17
11120500	San Jose	14·3	1140	1 Oct 1941–current	0·06
11120510	San Jose	24·4	1180	1 Oct 1970–30 Sep 2000	0·09

drains digitized from county and city drainage maps. The Soil Survey Geographic (SSURGO) Data Base (1995) for Santa Barbara County provides soils data for the top 2 m of soil. The current land use for this region was inferred from 1 : 42 000 scale aerial photographs taken in 1998 and classified based on Anderson Level III classifications (Anderson *et al*., 1976). To assess potential urbanization impacts on the measured streamflow time series (1988–2002), a 1986 land-use map (developed similarly to the 1998 land use) was also used. Monthly and annual precipitation contours were obtained from the parameter–elevation regressions on independent slopes model (PRISM; Daly *et al*., 1994) to evaluate the spatial distribution of rainfall within the watershed.

The study watersheds shown in Figure 2 were delineated using a 30 m DEM, modified to include the known locations of streams and storm drains (Moglen and Beighley, 2000). The delineation follows the rule that water will flow in the direction of the local gradient, making it possible to infer flow directions, flow lengths, slopes, drainage area, and watershed boundaries (O'Callaghan and Mark, 1984; Jenson and Domingue, 1988; Tarboton *et al*., 1991). Using the flow directions, a GIS layer of accumulated drainage area (i.e. flow accumulation) was determined. To identify the stream network, the flow accumulation layer was queried three times, highlighting all pixels draining more than 500, 1000, and 1500 pixels (0·45 km^2, 0·90 km^2, and 1·35 km^2) respectively). Based on a comparison between the threshold area drainage networks and the known stream locations, we selected the drainage network based on a threshold area of 1·35 km^2 (1500 pixels) and subdivided the watershed at all junctions within the inferred network.

Next, we quantified sub-area characteristics (such as elevation, local gradients, land uses, mean annual rainfall, saturated hydraulic conductivity, and available water storage) in the upper 2 m of soil. Topographic properties were obtained from the DEM. The distribution of land use was determined using 1998 land use. Mean annual rainfall was estimated using PRISM contours (Daly *et al*., 1994). Saturated hydraulic conductivity K_{sat}, and soil porosity, estimated as single depth-averaged values, were approximated using soil texture from SSURGO and conversions tables from Rawls *et al*. (1983). Available water storage was approximated using soil porosity and the average depth of soil above bedrock reported from SSURGO. Figure 4 shows the spatial distribution of three quantities: land use, slope and shallow bedrock. Table III provides summary statistics for the above sub-catchment hydrologic properties.

Because the HRU concept assumes the hydrologic properties are approximately homogeneous, sub-area characteristics were analysed for their internal spatial variability. However, making a quantitative assessment

Table III. Summary statistics for sub-area hydrologic properties, where A is drainage area, E is elevation, S is available water storage in upper 2 m of soil, K_{sat} is saturated hydraulic conductivity, and P is annual precipitation

Statistic	A (km^2)	E (m)	Slope (%)	S (cm)	K_{sat} (cm h^{-1})	P (cm)
Minimum	0·5	11	1	4	0·2	39
Maximum	4·2	935	52	69	3·9	68
Mean	1·7	266	22	36	1·1	49

of spatial variability for numerous hydrologic properties is a difficult task because of the varied data scales and hydrologic sensitivity. For our example, we selected seven measures of relevant hydrologic properties to assess HRU scale and homogeneity. The following measures represent ideal conditions, but conformity to such an extensive and varied list will likely be subjective: (1) the drainage area for each HRU should be less than 2·5 km^2; (2) the percentage of land surface within an HRU having a similar land use should be at least 70%; (3) the standard deviation of pixel elevations within an HRU should be less than 150 m (i.e. approximately 10% of the study area relief); (4) the standard deviation of annual precipitation within an HRU should be less than 3 cm (i.e. approximately 10% of the annual difference between mountain and coastal plain precipitation); (5) the percentage of land surface within an HRU having either steep (>20%) or moderate (<20%) slopes should be at least 60%; (6) the percentage of soils within an HRU having either high (>1 cm h^{-1}) or low (<1 cm h^{-1}) saturated hydraulic conductivity should be at least 70%; and (7) the percentage of HRU drainage area having either a known bedrock layer or none in the upper 2 m of soil should be at least 70%.

For the sub-catchments shown in Figure 2, the average drainage area was 1·7 km^2, ranging from 0·5 to 4·2 km^2. The average percentage of land surface with a similar land use was 84%, ranging from 45 to 100%. The average standard deviations for internal sub-area elevations and annual precipitation were 68 m and 1·5 cm, ranging from 5 to 200 m and 0 to 4·2 cm respectively. The average percentage of land surface with slopes in a single slope class was 83%. The average percentages of soils with similar saturated hydraulic conductivity and either a known bedrock layer or none were both 88%. Comparing these results with the above guidelines, approximately 8 of the 80 sub-areas were not in compliance for each rule. Given the generally favourable results, we continue our example using the inferred drainage network and corresponding sub-areas to represent our HRUs.

Next, we calculated various rainfall-runoff characteristics for the gauges shown in Figure 2. The Mediterranean climate concentrates more than 80% of the annual rainfall and runoff in the winter rainy season. The influence of only a few large annual rainfall events is evident, with the mean percentage of annual runoff produced by the annual maximum daily discharge ranging from 16 to 28% between gauges. The long-term, mean annual discharge ranges from 11 to 18 cm between gauges (i.e. 13 to 18% of annual rainfall is converted to runoff). Short, intense rainfalls drive a strongly pulsed runoff signal, with approximately 20% of the maximum daily discharge occurring in 1 h. Hydrograph recession rates are also rapid, with daily flow rates for the first and second days following the annual maximum discharge decreasing by approximately 72% and 89% respectively.

Overall, the watersheds have significant storage and loss mechanisms because only about 15% of the annual rainfall is converted to runoff, and following runoff events the streamflow quickly returns to near baseflow conditions. Based on these conditions, we qualitatively assign importance to streamflow components: surface runoff, interflow and groundwater. This is also consistent with our observed counterclockwise concentration–discharge relationship (Figure 3) for dissolved silica (Evans and Davies, 1998). Surface and/or interflow (i.e. shallow soil flow) must be dominant because of the rapid watershed response and hydrograph recession rates. Surface runoff is possible because of the limited soil storage in the upland regions and impervious surfaces in urban lands. Groundwater is less important, primarily providing baseflow, but it does contribute during larger runoff events. For all runoff excluding impervious runoff, there is significant storage when initial watershed conditions are dry (i.e. increasing runoff–rainfall ratios as the rainy season progresses).

Next, we investigate the available spatially distributed watershed data for uniqueness in space and compatibility with our hypotheses of dominant streamflow components and runoff mechanisms. Our data review and reasoning to this point suggest that both surface and subsurface runoff may occur, and that surface runoff is likely to vary between urban and rural lands and that subsurface runoff is likely either interflow from steep, shallow soils or groundwater from mildly sloping, deeper soils in the debris fans and coastal plain. Using an approach similar to defining HRUs, we focus on three sources of spatial data. First, land use is used to classify surface runoff as either urban or rural (Figure 4a). Next, the spatial distribution of subsurface runoff, either interflow or groundwater flow, is hypothesized based on presences of steep, shallow soils. Combining

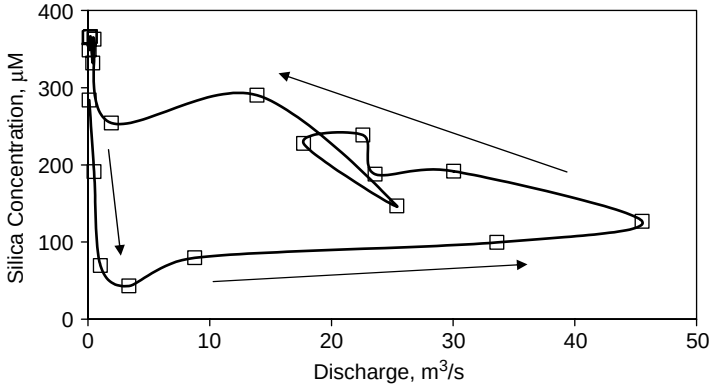

Figure 3. Concentration–discharge relationship for the outlet the Mission Creek watershed, 3–9 March, 2001, with arrows indicating the direction of hydrograph response (i.e. increasing time)

the data shown in Figure 4b and c, Figure 4d shows the distribution of regions having steep slopes ($\geq$20%) and a shallow bedrock layer (bedrock in the upper 2 m of soil); these are classified as interflow, with all other areas classified as groundwater runoff. For this example, the hypothesized distribution of runoff form is tested in the 'Hydrogeological evaluation, section using streamflow and instream silica concentrations.

Finally, we combine all the information and spatial coverages developed from the previous steps to assign dominant runoff components to each HRU, as illustrated in Figures 4e and f. Figure 4e shows HRUs classified as either urban (count = 41) or rural (count = 34), and Figure 4f shows the HRUs classified as either having interflow (count = 39) or groundwater (count = 36) runoff. Figures 4e and f were determined by overlaying Figures 4a and d on the HRU boundaries shown in Figure 2, and thus specifying the primary runoff components within each HRU. Although all HRUs containing shallow bedrock (i.e. 39 HRUs accounting for a land surface area of 76 km^2 or 60% of the 130 km^2 study area) have slope $\geq$20%, the slope threshold does not significantly impact the classification of interflow HRUs until slope reaches 30%. For example, using slopes of 25% and 30% reduces the number of interflow HRUs to 33 (67 km^2) and 24 (51 km^2) respectively.

By specifying only the dominant runoff processes in a particular HRU, the calculations to be done in that unit are limited, thus reducing the amount of required parameter estimation and the errors that would result from such estimations. Another benefit of the segregation and/or exclusion of certain processes in each HRU is that hypotheses of runoff processes and pathways can be clearly developed and tested against field observations. For example, discharge measurements and samples of shallow soil water, groundwater, surface runoff and streamflow can be collected from various HRUs, analysed for their corresponding chemical signatures and used to test the hypothesized spatial distribution of runoff form and behaviour. Focusing on dominant runoff processes also provides a conceptual simplification of basin hydrology that aids in transmitting model results to varied user groups. The following section highlights the usefulness of interpreting the spatial hydrogeological signature in hydrologic model development, parameterization and calibration.

Hydrologic model development

A rainfall-runoff model was developed, calibrated and used to simulate streamflow from four coastal watersheds in southern California for the period 1 September 1988 to 31 August 2002. The model utilizes a time step of 15 min and source-to-sink routing (Olivera and Maidment, 1999) to simulate streamflow at the watershed outlet and other points of interest (including the internal gauging locations). The model is spatially averaged at the HRU scale, enabling watershed-scale spatial patterns to be incorporated into the rainfall, runoff generation, and routing processes. Based on the approach of Jakeman and Hornberger (1993), the model is designed to simulate two runoff forms: surface and subsurface. Incorporating the hydrogeological

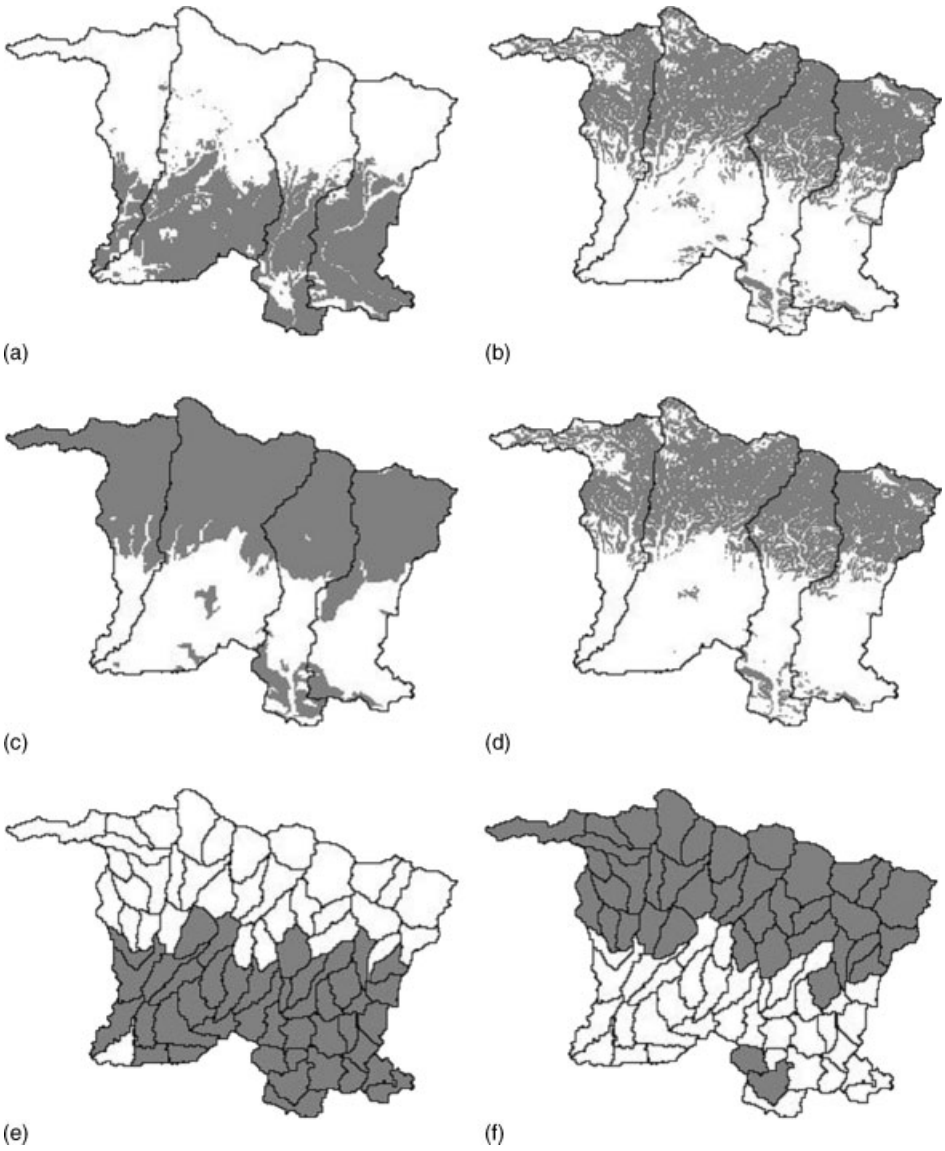

Figure 4. Spatial distribution of: (a) urban (grey) versus rural (white) land uses; (b) slopes $\geq$20% (grey) and $<$20% (white); (c) known bedrock layer in upper 2 m of soil (grey) or not (white); (d) interflow runoff (grey) and groundwater runoff (white) regions; (e) HRUs having urban surface runoff (grey) and HRUs having rural surface runoff (white); (f) HRUs having interflow runoff (grey) or HRUs having groundwater runoff (white)

interpretation, the two runoff forms are separated into two subclasses: (a) surface, i.e. urban or rural, and (b) subsurface, i.e. interflow or groundwater flow. Therefore, streamflow generated at the watershed outlets is comprised of runoff from potentially four sources, i.e. urban and rural surfaces, interflow and groundwater, whereas each HRU has the potential to contribute only two forms of runoff (i.e. surface and subsurface) because one possibility in each form has been eliminated based on the hydrogeological analysis. The modelling components for each form of runoff generation and routing are described below.

Conceptual runoff model. To model the rainfall-runoff processes, a two-component reservoir model was selected (Figure 5). Applying the mass balance of water to the control volumes shown in Figure 5 yields:

$$P_i(t) - P_{s,i}(t) - L_{s,i}(t) = \frac{dS_{s,i}(t)}{dt} \tag{1}$$

$$I_i(t) - L_{ss,i}(t) - Q_{ss,i}(t) = \frac{dS_{ss,i}(t)}{dt} \tag{2}$$

where subscripts 's,*i*' or 'ss,*i*' corresponding to surface and subsurface reservoirs respectively in a given HRU *i*; S_x [L^3] ($x =$'s,*i*' or 'ss,*i*,' is reservoir storage; P_i [L^3T^{-1}] is precipitation; $P_{s,i}$ [L^3T^{-1}] is precipitation available for infiltration and surface runoff; L_x [L^3T^{-1}] is storage losses; I_i [L^3T^{-1}] is infiltration; and Q_x [L^3T^{-1}] is runoff. For the storage loss term, the intent is to include the various physical loss mechanisms into one term in each store (e.g. evaporation and surface depressions for surface storage; deep groundwater recharge and evapotranspiration for subsurface storage). Combining Equations (1) and (2) and incorporating the relationship between surface runoff and infiltration, $Q_{s,i}(t) = P_{s,i}(t) - I_i(t)$, Equation (3) represents the combined surface and subsurface water balance:

$$Q_{s,i}(t) + Q_{ss,i}(t) = P_i(t) - L_{s,i}(t) - L_{ss,i}(t) - \frac{dS_{s,i}(t)}{dt} - \frac{dS_{ss,i}(t)}{dt} \tag{3}$$

Runoff generation. Runoff is generated from both the surface and subsurface. Surface runoff is generated under two conditions: when both the surface and subsurface storage reservoirs are full or when the rainfall occurs on an impervious surface. Subsurface runoff is generated when water is available in the subsurface reservoir. Because our approach utilizes the HRU concept, each HRU *i* has an initial and maximum storage reservoir capacity, and when precipitation begins, all rainfall goes toward filling the surface reservoir. Once the surface storage is satisfied, the precipitation not falling on impervious surfaces goes towards filling the subsurface reservoir, while all rainfall on impervious surfaces results in surface runoff. To summarize our

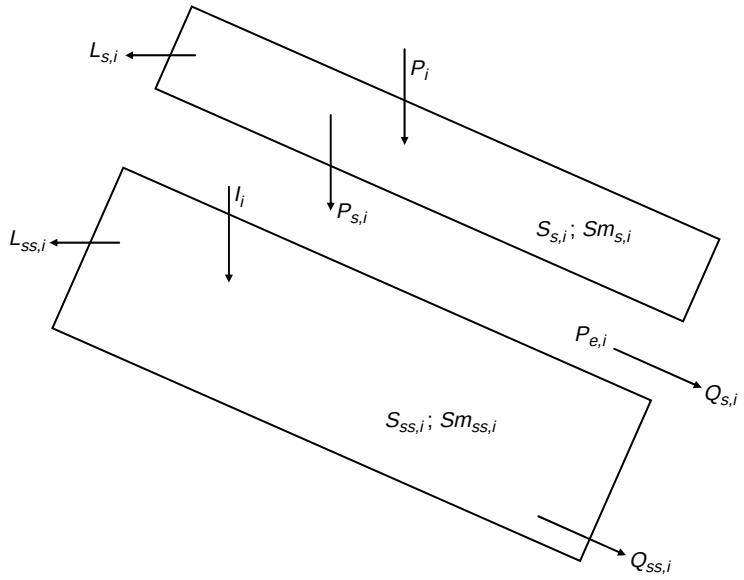

Figure 5. Rainfall-runoff model, where P_i is precipitation; $P_{s,i}$ is precipitation available for infiltration; $L_{s,i}$ and $L_{ss,i}$ are surface and subsurface losses respectively; $S_{x,i}$ and $Sm_{x,i}$ are existing and maximum storage capacity respectively, with x representing either surface (s) and subsurface (ss); I_i is infiltration; $P_{e,i}$ is excess precipitation; $Q_{s,i}$ is surface runoff; and $Q_{ss,i}$ is subsurface runoff for sub-area *i*, where subsurface represents either interflow or groundwater flow depending upon HRU characteristics

approach, the surface runoff rate or excess precipitation $P_{e,i}(t)$ [LT^{-1}], which is assumed uniformly distributed over HRU i, is determined by

$$P_{e,i}(t) = P_{s,i}(t) - I_i(t) \tag{4}$$

where $P_{s,i}(t)$ [LT^{-1}] is the precipitation rate to the subsurface storage reservoir in HRU i at time t and $I_i(t)$ [LT^{-1}] is the infiltration rate, both of which are determined conditionally:

$$P_{s,i}(t) = \begin{cases} 0 & \text{for} \quad S_{s,i}(t) < \mathrm{Sm}_{s,i} \\ P_i(t) - L_{s,i}(t) - \dfrac{\partial S_{s,i}}{\partial t} & \text{for} \quad S_{s,i}(t) = \mathrm{Sm}_{s,i} \end{cases} \tag{5}$$

$$I_i(t) = \begin{cases} (1 - U_i)P_{s,i}(t) & \text{for} \quad S_{ss,i}(t) < \mathrm{Sm}_{ss,i} \\ 0 & \text{for} \quad S_{ss,i}(t) = \mathrm{Sm}_{ss,i} \end{cases} \tag{6}$$

where $S_{x,i}(t)$ [L] is the surface or subsurface storage in HRU i at time t expressed in terms of depth, $\mathrm{Sm}_{x,i}$ [L] is the maximum surface or subsurface storage, and U_i is the percentage of impervious surface in HRU i. The rate of surface runoff is then converted to HRU runoff through routing, which is discussed in the next section.

Subsurface runoff is determined based on the inferred subsurface flow characteristics: interflow or groundwater flow. In both cases, the rate of subsurface runoff $\mathrm{Rs}_i(t)$ [LT^{-1}] is assumed uniformly distributed throughout the HRU, flowing in relation to the landscape gradient, and reaching the channel before being transmitted to the next downstream HRU:

$$\mathrm{Rs}_i(t) = \beta_i \left(S_{ss,i}(t)/\mathrm{Sm}_{ss,i}\right)^{\alpha_i} \tag{7}$$

where β_i and α_i are coefficients of the subsurface discharge affecting the magnitude and shape respectively (Sivapalan *et al*., 1996).

Runoff routing. Expanding upon the unit hydrograph model, Olivera and Maidment (1999) introduced a GIS-based spatially distributed flow routing algorithm called source-to-sink routing. Source-to-sink routing utilizes raster terrain data to infer a spatially distributed drainage network describing the connectivity between each grid cell. This network defines the flow path from any point (source) in a watershed to the overall outlet (sink). The source-to-sink routing model incorporates both advection and dispersion effects in each grid cell along the flow path from a source to its outlet, where the flow path is comprised of both upland (i.e. pixels not labelled as channels) and channel segments. For our application, a response hydrograph at a specific location or sink, $Q_i(t)$ [L^3T^{-1}], is then determined by summing all upstream contributions, which includes both surface and subsurface flow:

$$Q_i(t) = \sum_{j=1}^{n} Q_j(t) \tag{8}$$

where n is the number of sources and $Q_j(t)$ [L^3T^{-1}] is the combined discharge hydrograph from source j. The source hydrograph is determined by

$$Q_j(t) = A_j R_j(t) * u_j(t) \tag{9}$$

where A_j [L^2] is the area of source j, $R_j(t)$ [LT^{-1}] is the cumulative runoff rate (i.e. $P_{e,j}$ plus Rs_j) from source j, $u_j(t)$ [T^{-1}] is the response function from source j to sink i, and the asterisk represents the convolution integral.

The response function is a first-passage-time distribution:

$$u_j(t) = \frac{1}{2t\sqrt{\pi(t/t_j)/\Pi_j}} \exp\left\{-\frac{[1 - (t/t_j)]^2}{4(t/t_j)/\Pi_j}\right\} \tag{10}$$

where t_j [T] is the average flow time and Π_j is a representative Peclet number for the flow path (Olivera and Maidment, 1999). For conditions where the flow path from source j to sink i is comprised of path increments, the parameters for the whole path are determined by spatially weighting flow velocities, lengths and attenuation:

$$t_j = \sum_{k=1}^{m} \left(\frac{1}{v_k}\right) L_k \tag{11}$$

$$\Pi_j = \left[\sum_{k=1}^{m} \left(\frac{1}{v_k}\right) L_k\right]^2 \Big/ \sum_{k=1}^{m} \left(\frac{D_k}{v_k^3}\right) L_k \tag{12}$$

where m is the number of flow segments from source j to sink i, v_k [LT^{-1}] is the flow velocity, L_k [L] is the flow length, and D_k [L^2T^{-1}] is the attenuation coefficient for segment k.

The above routing describes two spatial units: source and segment. In the context of GIS and raster data, a source represents a continuous group of pixels draining to a common location (i.e. one pixel), and a flow segment is a single pixel or a series of pixels along the flow path from a source to its sink. The scale of a source can vary from one pixel to the entire watershed. In our case, delineated HRUs represent sources, USGS gauge locations (i.e. watershed outlets) represent sinks, and segments are individual pixels. Since we are using HRUs for sources, a representative flow path from the HRU centroid to its corresponding sink is used, where the flow path contains both overland (or subsurface for subsurface runoff) and channel pixels. Overland or subsurface pixels are those pixels not identified as stream cells in the gridded drainage network. Thus, the spatial patterns of velocity and attenuation are incorporated in the response function.

Model parameterization

Parameterization of the rainfall-runoff model was done in two steps. First, the watershed was subdivided and dominant hydrologic components were mapped and assigned to individual HRUs, as described previously. This process distributed HRU classifications for surface runoff (41 urban and 34 rural) and subsurface runoff (39 interflow and 36 groundwater), where rural lands were generally characterized as having interflow with 32 of 34 HRUs classified as rural also assigned to interflow (Figure 4). The benefit of this classification process is that the runoff mechanisms and pathways have been assigned to each HRU based on all available spatial and temporal data, reducing the likelihood of parameterizing non-existent runoff processes, while providing numerous quantitative measures useful for parameterization.

Next, model components were linked to the spatial and temporal databases using Visual Basic. In this process, the initial parameters values were estimated from the spatial/temporal data using guidelines based on the dominant runoff sources: (1) urban and rural surfaces and (2) interflow and groundwater flow. The first guideline pertains to maximum surface storage $Sm_{s,i}$. For HRUs classified as rural, $Sm_{s,i}$ was set to 1·3 cm to reflect the maximum initial losses for the dense shrub/brush land use predominant in the upland undeveloped areas (Viessman *et al*., 1977). For HRUs classified as urban, $Sm_{s,i}$ was set to 0·4 cm, which is typical for urban surface losses (Viessman *et al*., 1977). The impervious area in each HRU was estimated from the land-use coverage and lookup tables that relate land-use classification to percentage imperviousness (NRCS, 1986). The surface loss rate $L_{s,i}(t)$ in all HRUs was estimated as 0·4 cm day^{-1} based on surface evaporation rate typical for the winter rainy season along the Santa Barbara coast (California Irrigation Management Information System (CIMIS), http://wwwcimis.water.ca.gov/).

The second set of guidelines focused on the parameters for subsurface response: $Sm_{ss,i}$, $L_{ss,i}(t)$, β_i and α_i. As an initial estimate, the maximum subsurface storage capacity $Sm_{ss,i}$ was approximated as the maximum soil water capacity determined from the average depth of soil above bedrock (or total reported soil depth if no known bedrock layer) and porosity as reported from SSURGO. The loss rate from all subsurface storage reservoirs $L_{ss,i}(t)$ was set to 0·5 cm day^{-1} for interflow storage and 0·2 cm day^{-1} for groundwater

storage. The interflow loss rate was based on the estimated evaporation (ET) values (0·25 cm day^{-1}) for the mountains in winter months in southern California (CIMIS) plus assumed losses to deeper groundwater storage (0·25 cm day^{-1}). The groundwater loss rate was based on the estimated ET values (0·2 cm day^{-1}) for the coastal plain for winter months (CIMIS). The subsurface flow-rate parameters β_i and α_i affect the magnitude and shape respectively of the subsurface response rate (Equation (7)). To capture the magnitude and shape characteristics of the subsurface response, β_i and α_i were initially estimated from the average saturated hydraulic conductivity (cm h^{-1}) and ground slope (%) respectively. The logic for this initial approximation is based on: (a) the magnitude of the subsurface response being connected to the rate at which water enters the subsurface reservoir ($\beta \sim K_{sat}$); (b) the shape of the response being connected to the ground slope ($\alpha \sim S$), such that the slope of the response increases with increasing ground slope (i.e. as ground slope increases, the subsurface response reaches the maximum rate more rapidly). The large exponent, α_i equal to ground slope, in Equation (7) accounts for two subsurface response characteristics: (1) increasing subsurface flow rate with decreasing available storage and (2) non-effective storage (i.e. storage impacted by only ET and deeper groundwater losses). As the magnitude of α_i increases, so the percentage of available storage at which the subsurface response rate is approximately zero increases, thus representing the percentage of non-effective storage. For example, if $\alpha_i = 5$ (5% average ground slope), then the response rate is essentially zero when the ratio of current to maximum storage $S_{ss,i}(t)/\mathrm{Sm}_{ss,i} = 0{\cdot}25$, implying that 25% of the subsurface storage is non-effective. The subsurface flow rate can also be simulated with a modified version of Equation (7) using smaller values of α_i (e.g. 0·5 to 2) and subtracting the percentage of non-effective storage from both $S_{ss,i}(t)$ and $\mathrm{Sm}_{ss,i}$. In this application, the presented form of Equation (7) is used because it requires one less parameter (i.e. α_i accounts for both the shape of the response curve and non-effective storage). Table IV shows the initial and calibrated runoff parameters.

Three parameters, v_k, L_k, and D_k, are required for runoff routing. L_k was determined from the inferred drainage network, where L_k was the sum of both upland and channel segments. Two sets of velocity and attenuation values were used: upland (representing either surface or subsurface runoff rates along the flow path from the HRU centroid to its channel) and channel. Because of the relatively short distance of upland flow paths (less than 20% of channel lengths within an HRU and less than 5% of channel length to the corresponding watershed outlet) and the uncertainty in estimating/measuring subsurface flow parameters, the differences between overland and subsurface flow paths are neglected in this case study. Future efforts will focus more detail on this simplification. As initial estimates, upland flow velocity and attenuation were estimated as 0·15 m s^{-1} and 1·0 m^2 s^{-1} respectively and channel flow velocity and attenuation were estimated

Table IV. Initial and calibrated rainfall-runoff model parameters for: (a) urban and rural surfaces and (b) interflow and groundwater flow HRU classifications. Subscripts 's,*i*' and 'ss,*i*' correspond to surface and subsurface respectively, parameters in given HRU *i*, and parameter values for $\mathrm{Sm}_{ss,i}$, β_i and α_i represent: the mean and range within each HRU group for the initial parameterization and the adjustment factor for calibrated parameters (e.g. the calibrated β_i value for HRU *i* is either 1·3 or 1·5 times the initial parameter value for HRU *i*)

HRU component	$\mathrm{Sm}_{s,i}$ (cm)	$L_{s,i}$ (cm day^{-1})	$\mathrm{Sm}_{ss,i}$ (cm)	$L_{ss,i}$ (cm day^{-1})	β_i (cm h^{-1})	α_i
Initial parameter values						
Urban surfaces	0·3	0·4	n/a	n/a	n/a	n/a
Rural surface	1·3	0·4	n/a	n/a	n/a	n/a
Interflow	n/a	n/a	11 (4–20)	0·5	0·6 (0·2–2·4)	36 (18–52)
Groundwater flow	n/a	n/a	56 (38–69)	0·2	1·7 (0·8–3·9)	9 (1–22)
Calibrated parameter values						
Urban surfaces	0·6	0·6	n/a	n/a	n/a	n/a
Rural surface	1·9	0·6	n/a	n/a	n/a	n/a
Interflow	n/a	n/a	$1{\cdot}0 \times \mathrm{Sm}_{ss,i}$	0·6	$1{\cdot}3 \times \beta_i$	$0{\cdot}8 \times \alpha_i$
Groundwater flow	n/a	n/a	$0{\cdot}3 \times \mathrm{Sm}_{ss,i}$	0·2	$1{\cdot}5 \times \beta_i$	$0{\cdot}8 \times \alpha_i$

as 1·5 m s^{-1} and 140 m^2 s^{-1} respectively. The upland velocity was assumed to be a reasonable initial estimate, and the channel velocity was based on local, measured streamflow velocities. The attenuation estimates were based on Kashefipour and Falconer (2002). In addition to static variables, spatially and temporally distributed precipitation data are required to drive the model. In this study, data from eight gauges operated by Santa Barbara County Flood Control (Figure 2) were used to estimate 15 min precipitation time series for each HRU, $P_i(t)$ [LT^{-1}], based on HRU and gauge elevation. Given the uncertainty associated with all the above parameter estimations, a combination of sensitivity analysis and calibration was used to estimate a final parameter set.

Model calibration and verification

Rainfall-runoff parameters were calibrated for the period 1 September 1988 though to 31 August 1995 and verified for the period 1 September 1995 through to 31 August 2002 using 1998 land-use conditions. The 1998 land-use conditions are representative of the entire simulation period; there was essentially no change in land-use conditions between the 1986 and 1998 coverages. The intent of the following model calibration and verification is to demonstrate that our modelling approach (inferred from our hydrogeological interpretation) and spatial/temporal distribution of rainfall adequately reproduce streamflow for the 14 year simulation period.

The calibration period (1988–95) was selected as representative of the overall study period, with a mix of wet, dry and normal years. Although the watersheds contain 75 HRUs, the calibration process primarily focused on our sources of runoff: (1) urban and rural surfaces and (2) interflow and groundwater flow. Thus, 12 runoff parameters were used in the calibration process: four surface parameters ($Sm_{s,i}$ and $L_{s,i}$ for both urban and rural surfaces), two uniform subsurface parameters ($L_{ss,i}$ for both interflow and groundwater flow), six spatially distributed subsurface parameters ($Sm_{ss,i}$, β_i, and α_i for both interflow and groundwater flow), as shown in Table IV. Because the available data support the spatial distribution of $Sm_{ss,i}$, β_i, and α_i between HRUs, these parameters were adjusted uniformly within each subsurface group. For example, to evaluate the effects of β_i on interflow runoff response, β_i for each HRU classified as having interflow was increased or decreased by the same percentage of its initial estimate, thus preserving the spatial distribution of β_i, while providing feedback on the effects of magnitude change. For both the surface and subsurface storage reservoirs, the impacts on initial storage values were not significant. For all model runs, the model starts on 1 October, representing the end of the spring/summer dry season. Thus, the initial watershed conditions are very dry and the reservoirs are set to zero storage. The four routing parameters (velocity and attenuation for both upland and channel flow) were also calibrated/evaluated.

During the calibration process, model performance was assessed on the accuracy of annual maximum hourly discharge and annual runoff estimates using mean relative error RE

$$\mathrm{RE} = \left[\frac{1}{n}\sum_{i=1}^{n}\left(\frac{x_{o,i} - x_{s,i}}{x_{o,i}}\right)\right] \times 100 \tag{13}$$

and mean absolute error (AE)

$$\mathrm{AE}(\mathrm{m}^3\ \mathrm{s}^{-1}\ \text{or cm}\ ) = \frac{1}{n}\sum_{i=1}^{n}|x_{o,i} - x_{s,i}| \tag{14}$$

where $x_{o,i}$ is the measured value of either peak discharge or runoff depth, $x_{s,i}$ is the simulated value and n is the number of values being assessed. Because of frequent gauging errors and/or missing data, likely due to the rapid hydrograph response and extended dry periods, the available streamflow data were filtered. Although these issues are generally resolved or noted in the daily data provided by the USGS, our work required high resolution, provisional 15 min data. For example, the combined data series, representing 72 years of record (seven gauges; all available data for the entire 14 year period), contain only 34 years of complete data. On average, annual records were about 90% complete. Although missing data during non-storm events

are not significant, it was observed that gauges occasionally either stopped recording or reported unrealistic values during large runoff events. Since, the gauges are located within a few kilometres of each other, have similar watershed characteristics, and are generally subjected to similar rainfall, the filtering process focused on variations between gauges. For a given year, if the range in annual runoff (centimetres) between gauges exceeded the average value for all gauges in that year, then the outliers were eliminated until the range was less than the mean. This resulted in 16 of 72 annual runoff depths not being used. For example, in 1994, the data record for USGS gauge no. 11 119 940 was 85% complete with an annual runoff of 0·2 cm, whereas the other three active gauges had runoff depths of 2·6, 4·0 and 4·4 cm. Similarly, the annual maximum hourly discharges were filtered such that the range in peak discharge per unit area ($m^3\ s^{-1}\ km^{-2}$) was less than the mean, resulting in 18 of 72 peak discharges not being used in the error analysis. As an example, in 1990, the data record for USGS gauge no. 11 120 500 was 98% complete with a maximum hourly discharge of 0·002 $m^3\ s^{-1}\ km^{-2}$, whereas the other four active gauges had peak discharges of 0·11, 0·14, 0·16 and 0·17 $m^3\ s^{-1}\ km^{-2}$. The above filtering process also reduces the likelihood of having to calibrate peak discharges and runoff resulting from isolated patches of high- or low-intensity rainfall relative to our elevation-weighted precipitation, which is not the focus of this paper.

To minimize model error (i.e. mean RE and AE in peak discharges and runoff), parameter adjustment focused on three issues: (1) maximum storage capacity, (2) storage recovery rates, and (3) flow rates. The maximum storage capacity most notably affected model performance in dry conditions, when it can be assumed that the initial storage conditions are near zero (i.e. capacity to store water is at a maximum). The storage recovery rates affected model performance during a series of storms, and the flow rates (routing velocity and subsurface flow parameters β_i and α_i) affected peak discharge estimates. To illustrate the above concepts and general model performance, simulated and measured hydrographs for two storms in water year 2001 for Mission Creek (USGS no. 11 119 750) are shown in Figure 6. These two storms were selected to highlight the impacts of dry (i.e. early part of rainy season) versus wet conditions. The January response ($Q_p = 9{\cdot}8\ m^3\ s^{-1}$ and 2·9 cm of runoff) was generated from approximately 15 cm of rainfall, and the March response ($Q_p = 38{\cdot}9\ m^3\ s^{-1}$ and 11·3 cm of runoff) resulted from 19 cm of rainfall. Although the difference in rainfall was only 11%, the difference in runoff was 74% because of the watershed conditions prior to each event. The January event was essentially the first storm of the water year, whereas the March storm was the last, thus highlighting the importance of available storage capacity.

For evaluating model performance, the hydrographs shown in Figure 6 are separated into three components: (1) rising, (2) peaks and (3) recession. In both Figure 6a and b, the initial rise of the hydrograph agrees well with the observed data. The initial rise of the simulated hydrograph in Figure 6a is slightly ahead of the observed rise. The opposite is the case in Figure 6b. The timing of the initial rise is most sensitive to the available storage at the onset of the rainfall event. The peak and/or peaks of the hydrographs tend to be impacted by the available rainfall data. Once the watershed is responding, the high relief and shallow bedrock tends to transmit the rainfall signal rapidly to the outlet of the watershed. Therefore, the internal peaks of the hydrographs were assigned less weight when assessing overall model performance. For example, Figure 6a shows a second peak on 11 January 2001 that is not present in the observed data. The third component, hydrograph recession, was the most difficult to simulate, reflecting the complexity of the processes and pathways associated with primarily subsurface flow. In Figure 6a, the model overestimates the recession limb, whereas Figure 6b shows that the model underestimates the recession, suggesting a seasonal influence on the recession characteristics. In light of the sensitivity of the model to available rainfall data, the hydrographs in Figure 6 indicate the applicability of the model and our hypothesized distribution of dominant runoff sources.

Table V provides the calibrated model parameters. Although the calibrated parameters are similar to their initial estimates, the adjustments generally reduced predicted peak discharge and runoff depth. Prior to calibration, the mean error for the annual maximum hourly discharge Q_p, for the seven gauges was −47% (17·2 $m^3\ s^{-1}$), ranging from −113 to −14% (5·4 to 30·5 $m^3\ s^{-1}$) between gauges, and the mean error in annual runoff was −28% (3·1 cm), ranging from −41 to −9% (0·7 to 5·1 cm) between gauges. After calibration, the mean error in Q_p for the seven gauges was −2% (9·2 $m^3\ s^{-1}$) ranging from −16 to +10% (0·3 to

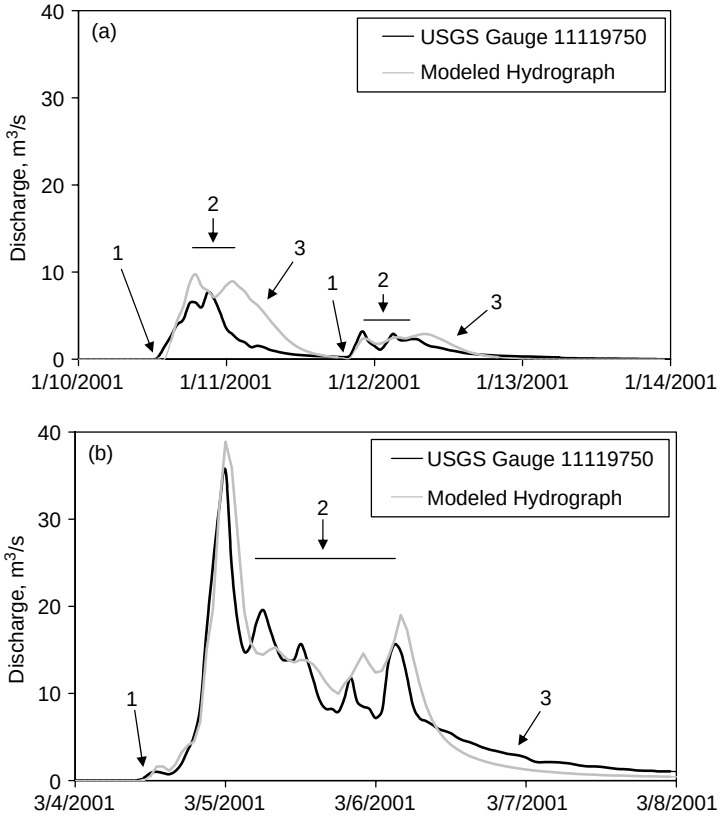

Figure 6. Modelled and observed streamflow hydrographs for two storms from water year 2001 in Mission Creek (USGS gauge no. 11119750): (a) 10–14 January 2001 and (b) 4–8 March 2001, with nos 1–3 corresponding to hydrograph features (initial rise, peaks and recession respectively) discussed in the text

Table V. Model calibration statistics for water years 1989–95, where the mean, minimum and maximum peak discharges Q_p and mean annual runoff depth (RO) are from the measured data, and the relative error (RE) and absolute error (AE) represent average errors for individual peak discharges and annual runoff from each water year simulated (gauge 11 119 745 not active)

Summary statistic	11119750	11119780	11119940	11120000	11120500	11120510	All gauges
Mean Q_p (m^3 s^{-1})	28·8	22·1	33·4	88·5	15·0	20·6	39·4
Min Q_p (m^3 s^{-1})	2·9	22·1	1·1	8·6	0·7	2·3	0·7
Max Q_p (m^3 s^{-1})	130·5	22·1	80·0	203·7	37·4	54·8	203·7
RE, Q_p (%)	−14·4	1·4	10·2	4·5	−15·6	6·9	−2·0
AE, Q_p (m^3 s^{-1})	10·3	0·3	10·3	14·7	6·0	3·5	9·2
Mean RO (cm)	13·9	10·1	26·2	19·6	10·5	4·3	15·4
RE, RO (%)	5·4	8·6	−4·6	−15·1	24·9	7·5	2·6
AE, RO (cm)	3·6	0·7	3·5	3·1	2·7	0·7	2·7

14·7 m^3 s^{-1}) between gauges, and the mean error in annual runoff was 3% (2·7 cm), ranging from −15 to +25% (0·7 to 3·6 cm) between gauges (Table VI). Although the average relative error in runoff at gauge 11 120 500 (25%) might be considered excessive, the mean absolute error was only 2·7 cm. Overall, model errors were generally favourable, providing support for the calibration and modelling approach.

Table VI. Model validation statistics for water years 1996–2002, where the mean, minimum and maximum peak discharges Q_p and mean annual runoff (RO) are from the measured data, and the relative error (RE) and absolute error (AE) represent average errors for individual peak discharges and annual runoff from each water year simulated (gauge 11 119 780 not active)

Summary statistic	11119745	11119750	11119940	11120000	11120500	11120510	All gauges
Mean Q_p (m^3 s^{-1})	7·6	24·7	22·2	71·8	24·0	36·0	34·1
Min Q_p (m^3 s^{-1})	0·9	2·8	1·6	8·4	1·1	4·4	0·9
Max Q_p (m^3 s^{-1})	14·3	79·2	56·7	260·9	64·2	67·7	260·9
RE, Q_p (%)	−23·7	16·5	−25·9	−2·6	15·2	23·1	0·1
AE, Q_p (m^3 s^{-1})	16·1	7·0	8·1	37·2	8·7	1·2	14·5
Mean RO (cm)	16·4	13·5	16·1	28·4	18·7	28·0	19·4
RE, RO (%)	36·3	11·1	−23·5	24·8	26·3	35·3	12·7
AE, RO (cm)	5·0	3·2	3·1	7·3	3·8	9·1	4·9

To validate the calibrated model parameters, streamflow was simulated for the period 1 September 1995 through to 31 August 2002. For peak discharge, the model performance for the validation period is similar to the calibration period; for runoff depth, the model performance is less favourable (mean error in annual runoff was 13% or 4·9 cm) but still reasonable (Table VI). For the entire 14 year period, the initial parameter estimates resulted in mean errors in peak discharge and runoff volume of −50% (17·2 m^3 s^{-1}) and −23% (4·6 cm) respectively, and the calibrated parameter set resulted in mean errors in peak discharge and runoff volume of −1% (11·9 m^3 s^{-1}) and −8% (3·8 cm) respectively. Although the percentage error in peak discharge for the initial parameter set seems excessive, the absolute errors indicate that our parameterization approach is effective. The overall generally favourable results indicate that the model can be used to simulate streamflow from varying land uses (urban and non-urban) and climatic conditions (wet and dry years). The probable differences between measured and inferred rainfall, stream gauge error, and simplified complexities of the system imply a certain level of modelling uncertainty, but the intent of the calibration/validation process was not to match each hydrograph exactly, rather it was to assess whether our inferred spatial distribution of runoff form and behaviour based on the hydrogeological interpretation is plausible. In the next section we use instream silica concentrations to evaluate further our inferred distribution of dominant runoff processes.

Hydrogeological evaluation

We have shown that our hydrogeological interpretation provides a logical basis for partitioning the landscape into regions of similar runoff components and for developing, parameterizing and calibrating a rainfall-runoff model. Based on this interpretation, we suggest that our approach provides a faithful representation of the spatial distribution of runoff processes and pathways. However, our model evaluation relies primarily on streamflow data. Although streamflow has an inherent structure that provides insight into its composition, it is difficult to assess model performance adequately for individual runoff components (i.e. surface and subsurface) using only streamflow. To support our research, focused on correctly inferring individual sources of runoff by decoupling the landscape's hydrogeological signature, we used instream silica concentrations to assess the contributions of surface, interflow and groundwater runoff from our model.

Scanlon *et al*. (2001) show that silica concentration is noticeably different between surface water, groundwater and shallow soil water, building on the earlier work by Pinder and Jones (1969) that focused on only two sources, i.e. on surface water and groundwater. This difference can be incorporated into an end-member mixing model:

$$C_T = \frac{C_s Q_s + C_{ss} Q_{ss} + C_{gw} Q_{gw}}{Q_T} \tag{15}$$

where C is silica concentration and Q is flow, with the subscripts representing surface runoff (s), ('interflow') shallow soil flow (ss), groundwater flow (gw), and the combined stream flow (T). In addition to the difference

between interflow and groundwater flow, Scanlon *et al*. (2001) indicate that the surface runoff has a minimal silica concentration. Thus, if silica concentrations can be estimated for the three runoff sources, then it is possible to simulate stream silica concentrations using predicted streamflow components and Equation (15). For our study region, the groundwater concentration was estimated by analysing streamflow samples taken at the end of extended dry periods (i.e. when all flow is likely to be from groundwater sources). Interflow silica concentration was then bracketed between near zero and the groundwater levels. To tighten this bracket, field measurements of interflow silica concentration are required. However, measuring interflow at point locations requires additional assumptions regarding the spatial and temporal distribution at the modelling unit scale.

Combining our three simulated runoff components with assumed silica concentration for surface, interflow and groundwater runoff, stream silica concentrations were estimated. For example, Figure 7 shows predicted and measured stream silica concentrations in Mission Creek for 4–7 March 2001. The groundwater silica concentration was estimated as 350 μM from measurements taken during baseflow conditions. The surface and interflow concentrations were estimated as 44 μM and 263 μM respectively, based on 12% and 65% respectively of the groundwater concentration. Although these percentages are based on Scanlon *et al*. (2001) and not measured data, the timing of the simulated runoff components combined with measured streamflow characteristics and the temporal pattern of measured silica concentrations suggests that our estimated surface and soil water concentrations are reasonable. For example, in urban areas, where surface runoff dominates the initial hydrograph rise, silica concentrations range from 10 to 100 μM. In upland areas, where interflow dominates hydrograph peaks, silica concentrations range from 225 to 275 μM. For the silica predictions shown in Figure 7, the average error between the measured and simulated silica concentrations was 5·9%. For all of 2001, a total of 95 measured stream silica concentrations were available for Arroyo Burro (59) and Mission (36) creeks. Using the above procedure, stream silica concentrations were estimated for all 95 samples. The results were good, with mean errors of 2·8% (5·5 μM) for Arroyo Burro and −2·1% (8·6 μM) for Mission Creek. Although our research and field sampling efforts are continuing, the favourable agreement between the

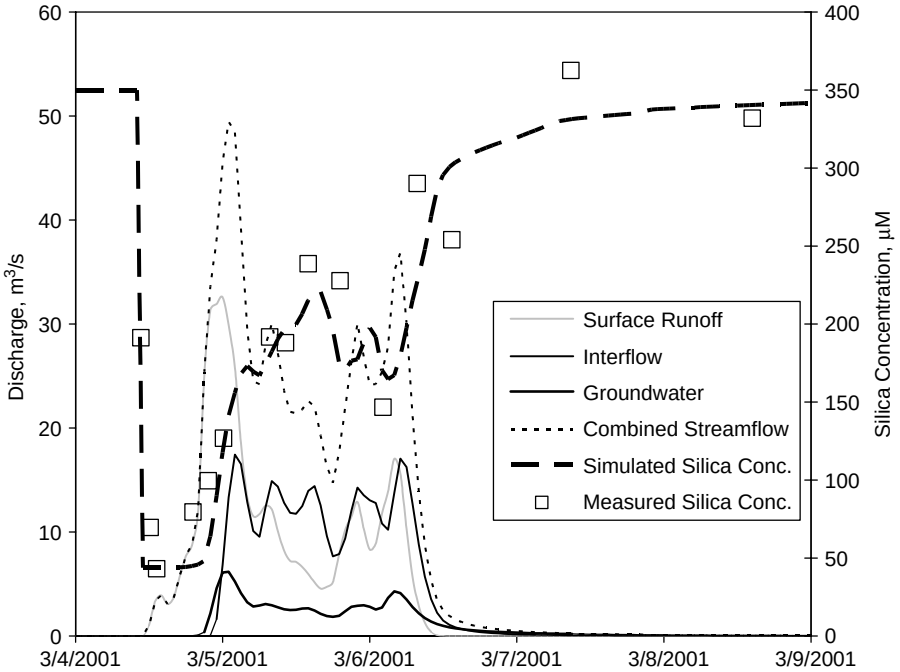

Figure 7. Simulated storm hydrograph and individual runoff components (surfaces, interflow, and groundwater) with measured and simulated stream silica concentrations for Mission Creek, 4–9 March 2001

measured and estimated silica concentrations suggests that our overall modelling approach and hydrogeological interpretation is applicable.

CONCLUSIONS

We presented an approach for modelling basin hydrology that integrates HRU concepts and hydrogeological interpretation, applicable for both existing and new models. Our approach focuses on determining the fundamental hydrologic components of a basin and mapping areas that are expected to exhibit similar runoff mechanisms and pathways. Combining our approach with existing HRU concepts, we present a new basin-scale model that simulates streamflow from three sources of runoff: surface, interflow and groundwater. A case study, of four watersheds draining the southern coast of California near Santa Barbara, is presented to demonstrate our hydrogeological interpretation and modelling approach.

The two primary benefits of our enhanced HRU modelling approach are: (1) clearly defined hypotheses for the spatial distribution of dominant runoff mechanisms and pathways testable against field observations and (2) limited over-parameterization. The combination of streamflow hydrographs and instream silica concentrations was used to show how the inferred spatial distribution of runoff mechanisms agrees with observed conditions. Using streamflow data, the model performed well throughout the entire 14 year period, with mean errors in peak discharge and runoff volume of -1% ($11{\cdot}9$ m^3 s^{-1}) and -8% ($3{\cdot}8$ cm) respectively. Because our approach focuses on dominant runoff components, we were able to utilize measured stream silica concentrations to assess the primary sources of basin runoff: overland, interflow and groundwater flow. Based on our simulated sources of runoff, we were able to predict stream silica concentrations accurately, with mean errors of $2{\cdot}8\%$ ($5{\cdot}5$ μM) in Arroyo Burro and $-2{\cdot}1\%$ ($8{\cdot}6$ μM) in Mission Creeks.

By grouping the watershed into regions of similar runoff and by focusing our spatial analysis on specific runoff processes, we reduce the parameterization and calibration of non-existent processes, while providing physically meaningful, quantitative measures that aid in characterizing the inferred processes. The calibration process also benefits from our partitioning HRUs based on their inferred runoff components, because parameter adjustments are constrained to uniform adjustments that include all HRUs with similar runoff processes rather than individual parameters in each HRU, vastly reducing the number of potential adjustments. Although the model results for the entire 14 year period using our initial parameter estimates (mean errors in peak discharge and runoff volume were -50% ($17{\cdot}2$ m^3 s^{-1}) and -23% ($4{\cdot}6$ cm) respectively) were marginal, the similarity of our initial and calibrated parameter sets suggests that initial model parameters can be estimated from tables, available data and hydrologic reasoning.

While our case study focused on a new conceptual model that we constructed for the purpose of tracking numerous runoff components in the combined streamflow, our concepts are also applicable for existing, spatially averaged, models. In addition to the primary benefits listed above, our study illustrates other favourable aspects of hydrogeological interpretation, such as: providing a rational basis for the selection of applicable runoff mechanisms; supporting a modelling framework that focuses on the fundamental components of basin hydrology; and increasing awareness of individual sources of runoff, rather than relying on only combined streamflow for model evaluation. Our hydrogeological interpretation can be incorporated into standard modelling procedures, providing direction for future research efforts to improve understanding of fundamental basin hydrology. Our approach for mapping the spatial distribution of runoff mechanisms and components is particularly relevant for water quantity and quality studies, because it forces modellers and managers to quantify the spatial extent of similar runoff (and contamination) characteristics before initiating the modelling process.

ACKNOWLEDGMENTS

This research was conducted as part of the Santa Barbara Channel–Long Term Ecological Research Project supported by the National Science Foundation under Cooperative Agreement No. OCE-9982105.

We acknowledge the Mesoscale Effects of Climate and Land-Cover Change on River-Basin Hydrology in Amazonia Project supported by the National Aeronautics and Space Administration under Cooperative Agreement No. NAG5-8396 for providing added research focus. We also thank the Santa Barbara County Public Works Department and the USGS for their generous sharing of data.

REFERENCES

Anderson JR, Hardy EE, Roach JT, Witmer RE, 1976. *A land use and land cover classification system for use with remote sensor data*. US Geological Survey, Professional Paper 964. USGS, Reston, VA.

Arnold JG, Williams JR, Maidment DR. 1995. Continuous-time water and sediment-routing model for large basins. *Journal of Hydraulic Engineering* **121**(2): 171–183.

Becker A, Braun P. 1999. Disaggregation, aggregation and spatial scaling in hydrological modeling. *Journal of Hydrology* **217**: 239–252.

Beven KJ. 2001. *Rainfall-Runoff Modelling, The Primer*. John Wiley: Chichester.

Daly C, Neilson RP, Phillips DL. 1994. A statistical–topographic model for mapping climatological precipitation over mountainous terrain. *Journal of Applied Meteorology* **33**: 140–158.

Donigian ASD, Bicknell BR, Imhoff JC. 1995. Hydrologic simulation program—Fortran. In *Computer Models of Watershed Hydrology*, Singh VP (ed.). Water Resources Publications: Highlands Ranch, CO; 395–442.

Evans C, Davies TD. 1998. Causes of concentration/discharge hysteresis and its potential as a tool for analysis of episode hydrochemistry. *Water Resources Research* **34**(1): 129–137.

Farvolden RN. 1963. Geologic controls on ground-water storage and base flow. *Journal of Hydrology* **1**(3): 219–249.

Grayson RB, Blöschl G. 2000. Summary of pattern comparison and concluding remarks. In *Spatial Patterns in Catchment Hydrology: Observations and Modeling*, Grayson RB, Blöschl G (eds). Cambridge University Press: 355–367.

Grayson RB, Blöschl G, Western AW, McMahon TA. 2002. Advances in the use of observed spatial patterns of catchment hydrological response. *Advances in Water Resources* **25**: 1313–1334.

Gremillion P, Gonyeau A, Wanielista M. 2000. Application of alternative hydrograph separation models to detect changes in flow paths in a watershed undergoing urban development. *Hydrological Processes* **14**: 1485–1501.

Harr RD. 1977. Water flux in soil and subsoil on a steep forested slope. *Journal of Hydrology* **33**(1–2): 37–58.

Hellie F, Peschke G, Seidler C, Niedel D. 2002. Process-oriented subdivision of basins to improve the preprocessing of distributed precipitation-runoff-models. In *Interdisciplinary Approaches in Small Catchment Hydrology: Monitoring and Research, Proceedings of the 9th Conference of the European Network of Experimental and Representative Basins*, Holko L, Miklanek P (eds). Demanovska dolina, Slovakia.

Hewlett JD, Hibbert AR. 1963. Moisture and energy conditions within a sloping soil mass during drainage. *Journal of Geophysical Research* **68**(4): 1081–1087.

Hoeg S, Uhlenbrook S, Leibundgut C. 2000. Hydrograph separation in a mountainous catchment—combining hydrochemical and isotopic tracers. *Hydrologic Processes* **14**: 1199–1216.

Jakeman AJ, Hornberger GM. 1993. How much complexity is warranted in a rainfall-runoff model? *Water Resources Research* **29**(8): 2637–2649.

Jensen SK, Domingue JO. 1988. Extracting topographic structure from digital elevation data for geographic system analysis. *Photogrammetric Engineering and Remote Sensing* **54**(11): 1593–1600.

Kashefipour SM, Falconer RA. 2002. Longitudinal dispersion coefficients in natural channels. *Water Research* **36**: 1596–1608.

Ladouche B, Probst A, Viville D, Idir S, Baque D, Loubet M, Probst JL, Bariac T. 2001. Hydrograph separation using isotopic, chemical and hydrological approaches (Stengbach catchment, France). *Journal of Hydrology* **242**: 255–274.

Liang X, Lettenmaier DP, Wood EF, Burges SJ. 1994. A simple hydrologically based model of land surface water and energy fluxes for GSMs. *Journal of Geophysical Research* **99**(D7): 14 415–14 428.

Miller SN, Kepner WG, Mehaffey MH, Hernandez M, Miller RC, Goodrich DC, Devonald KK, Heggem DT, Miller WP. 2002. Integrating landscape assessment and hydrologic modeling for land cover change analysis. *Journal of the American Water Resources Association* **38**(4): 915–929.

Moglen GE, Beighley RE. 2000. Using GIS to determine extent of gauged streams in a region. *ASCE Journal of Hydrologic Engineering* **5**(2): 190–196.

Moglen GE, Kosicki A. 2000. Research pays off: GISHydro2000: performing automated hydrologic analysis in Maryland, Transportation Research Board, National Research Council. *Transportation Research News* **210**: 18–19.

National Hydrography Dataset. 1999. *The National Hydrography Dataset*. US Geological Survey, Fact Sheet 106–99. USGS, Reston, VA.

NOAA. 2001. *Sulphur Mountain Doppler radar: a performance study*, NOAA Technical Memorandum NWS WR-267. US Department of Commerce, National Oceanic and Atmospheric Administration, National Weather Service, Los Angeles Weather Service Office, Oxnard, CA.

NRCS. 1986. *Urban hydrology for small watersheds*. Technical Release 55. Natural Resources Conservation Service, Washington, DC.

Olivera F. 2001. Extracting hydrologic information from spatial data for HMS modeling. *ASCE Journal of Hydrologic Engineering* **6**(6): 524–530.

Olivera F, Maidment D. 1999. Geographic information systems (GIS)-based spatially distributed model for runoff routing. *Water Resources Research* **35**(4): 1155–1164.

O'Callaghan JF, Mark DM. 1984. The extraction of drainage networks from digital elevation data. *Computer Vision, Graphics and Image Processing* **28**: 323–344.

Peschke G, Etzenberg C, Muller G, Topfer J, Zimmermann S. 1999. Runoff generation regionalization—analysis and a possible approach to a solution. In *Regionalization in Hydrology*, Bernd D, Kirkby MJ, Schroder U (eds). IAHS Publication No. 254. IAHS Press: Wallingford; 147–156.

Pinder GF, Jones JF. 1969. Determination of the groundwater component of peak discharge from the chemistry of total runoff. *Water Resources Research* **5**: 438–445.

Rawls WJ, Brakensiek DL, Miller N. 1983. Green–Ampt infiltration parameters from soils data. *ASCE Journal of Hydraulic Engineering* **109**(1): 62–70.

Scanlon TM, Raffensperger JP, Hornberger GM. 2001. Modeling transport of dissolved silica in a forested headwater catchment: implications for defining the hydrochemical response of observed flow pathways. *Water Resources Research* **37**(4): 1071–1082.

Sivapalan M, Ruprecht JK, Viney NR. 1996. Water and salt balance modelling to predict the effects of land use change in forested catchments. 1. Small catchment water balance model. *Hydrological Processes* **10**: 393–411.

Soil Survey Geographic (SSURGO) Data Base. 1995. *Data user information*. Miscellaneous Publication Number 1527. United States Department of Agriculture, National Resources Conservation Service, National Soil Survey Center.

Tarboton DG, Bras RL, Rodriguez-Iturbe I. 1991. On the extraction of channel networks from digital elevation data. *Hydrological Processes* **5**: 81–100.

USACE. 2000. *HEC-HMS technical reference manual*. United States Army Corps of Engineers, Hydrologic Engineering Center, Davis, CA.

Viessman W, Knapp JW, Lewis GL, Harbaugh TE. 1977. *Introduction to Hydrology*. Harper and Row: New York.

Woods RA. 2002. Seeing catchments with new eyes. Spatial patterns in catchment hydrology: observations and modeling. *Hydrological Processes* **16**(5): 1111–1113.

Wooldridge SA, Kalma JD, Franks SW, Kuczera G. 2002. Model identification by space–time disaggregation: a case study from eastern Australia. *Hydrological Processes* **16**(2): 459–477.

